THESIS FOR THE DEGREE OF DOCTOR OF PHILOSOPHY IN SOLID AND STRUCTURAL MECHANICS

Dynamic response reconstruction using passive components

ANDERS T. JOHANSSON

Department of Applied Mechanics
CHALMERS UNIVERSITY OF TECHNOLOGY

Gothenburg, Sweden 2012

Dynamic response reconstruction using passive components
ANDERS T. JOHANSSON
ISBN 978-91-7385-681-2

Doktorsavhandlingar vid Chalmers tekniska högskola
Ny serie nr. 3362
ISSN 0346-718X
Department of Applied Mechanics
Chalmers University of Technology
SE-412 96 Gothenburg
Sweden
Telephone: +46 (0)31-772 1000

Cover:
Example of passive control concept: Linear system on state-space form modified by a passive control component.

Chalmers Reproservice
Gothenburg, Sweden 2012

Dynamic response reconstruction using passive components
Thesis for the degree of Doctor of Philosophy in Solid and Structural Mechanics
ANDERS T. JOHANSSON
Department of Applied Mechanics
Chalmers University of Technology

Abstract

In many testing applications within the field of structural dynamics, such as noise and vibration harshness, rattle and squeak, or durability testing in the automotive and truck industries, large hydraulic or electromagnetic actuators are used to excite the tested structure. Such actuators are mounted in the laboratory in a fixed configuration referred to here as a test rig.

A frequent method for calculating the input to such test rigs is to replicate a certain reference signal, for instance dynamic responses from driving tests, to ensure that the test case is physically motivated. Versions of the Time Waveform Replication (TWR) method are often used to this end, iteratively calculating an input sequence used to excite a system such that its response replicates a desired reference. The TWR algorithm essentially estimates the unknown input by pseudo-inversion of the frequency domain transfer function.

In most situations, TWR will ensure a test output which is close to the reference signal; however, if there are eigenmodes of the test specimen in the desired frequency range of the test which are uncontrollable, it can be shown that the required input force and/or the error between test output and desired reference will be large. Such problems remain even when reference-contributing modes are but marginally controllable. In a test rig such as described above, this controllability shortcoming may be impossible to prevent in the usual manner, *i.e.* through changing the input configuration. This can cause poor reference replication whereby the validity of the test may be put into question.

For such specific cases, where the possibilities of changing the input configuration is slim and controllability is lacking, a different approach is required. This thesis presents such an approach. It introduces the concept of passive control to the problem of response reconstruction: By attaching a modifying component to the tested structure, designed specifically to improve response reconstruction, the controllability of the system can improve.

Two methods for designing such passive components are described. The first uses a high-quality finite element model of the tested structure and parameterized passive component, performing synthetic TWR experiments to evaluate its rig control properties. The second uses instead an experimentally derived model of the tested structure, which is coupled to the analytical model of the passive component through an experimental/analytical substructuring technique.

Keywords: experimental methods, Time Waveform Replication, response reconstruction, drive signal identification, passive control, model calibration, model updating, substructuring, controllability

to my family, to what use they may put it.

If you'd like to gamble, I'll tell you how it ends
You win some, lose some, it's all the same to me

♠

Preface

The work presented in this thesis was carried out during the period June 2006 - May 2012 as a part of a research project at the Department of Applied Mechanics at Chalmers University of Technology. The project is financially supported by a donation from the Ekman foundation (Ekmanska stiftelsen). This support is gratefully acknowledged.

I would like to take this opportunity to express my sincere gratitude to my supervisor Prof. Thomas Abrahamsson, whom has given excellent supervision, always ready to discuss and give input to the work as well as read and give feedback on manuscripts. I would also like to thank my co-supervisor Prof. Tomas McKelvey, who's knowledge in system identification and signal processing has been a great resource in the course of this work. Research engineer Jan Möller, who has realized the passive components used in the experimental work and assisted in their attachment and reattachment with superhuman patience; thank you. I am also grateful to the people at Volvo Group Trucks Technology, notably Magnus Larsson, Dr. Magnus Karlsson and Inge Johansson for their patience in introducing me to the workings of real test rigs.

The quality of this thesis, such as it is, also owes to the thorough scrutiny it was being put to by Ass. Prof. Matthew Allen in the screening process prior to my dissertation. This identified several issues that could be addressed prior to printing, for which I am very grateful.

I became interested in research when writing my master's thesis at the TU Delft, under Prof. Fred van Keulen. Therefore, and for his contributions to the first paper of this thesis, I would like to thank him and his colleagues at the SOCM group. I would also like to thank Björn Pålsson for ushering me to the Netherlands in the first place, and also for fruitful discussions mainly on topics of optimization.

I appreciate all of my colleagues, past and present, for their support, and for creating an enjoyable work space. Some of these colleagues have furthermore contributed to the work in this thesis: Therefore, thanks to Dr. Per Sjövall, for support in the implementation of his coupling methods, Anders Liljerehn, for fruitful discussions of said coupling methods and Dr. Jonathan Westlund, for advice in questions of mathematics. Several others have contributed as well, but I think that sums up the main part.

Working with research can be very frustrating. For helping me blow of some steam, I'd like to thank all of my friends, especially Rackarnas BK, ride 'em on down and the people of the Orust annual Bon Scott fiesta.

Last, I'd like to thank my family - my parents, siblings, wife and kids - for their invaluable support during the work of this thesis. I love you.

Gothenburg, April 2012

Anders T. Johansson

Thesis

This thesis consists of an extended summary and the following appended papers:

Paper A	A. T. Johansson, T. J. S. Abrahamsson, and F van Keulen. "Comparison of several error metrics for FE model updating". *Proceedings of IMAC XXV, the International Modal Analysis Conference.* 2007
Paper B	A. T. Johansson and T. J. S. Abrahamsson. "Increased controllability in component testing using structural modifications". *Proceedings of ISMA 2008 the International Conference on Noise and Vibration Engineering.* 2008
Paper C	A. T. Johansson and T. J. S. Abrahamsson. *A method for improving test rig performance using passive components.* Submitted for international publication. 2012
Paper D	A. T. Johansson and T. J. S. Abrahamsson. *Application of passive components for improved tracking in controllability-lacking test rigs.* Submitted for international publication. 2012
Paper E	A. T. Johansson and T. J. S. Abrahamsson. "An experimental approach to improve controllability in test rigs using passive components". *Submitted to ISMA 2012 the International Conference on Noise and Vibration Engineering.* 2012

The appended papers were prepared in collaboration with co-authors. The author of this thesis was responsible for the major progress of work, *i.e.* planning the papers, developing the theory, developing and carrying out the numerical implementations and simulations, performing the experiments and writing the papers.

Contents

Abstract i

Preface v

Thesis vii

Contents ix

I Extended Summary 1

1 Introduction and motivation 1

2 Models in structural dynamics 2
2.1 External description 2
2.2 Internal description 4
2.3 Parametric model calibration 6

3 Time Waveform Replication 7
3.1 TWR in industry 8
3.2 Contraction mapping and convergence 9
3.3 Drive signal generation methods 11
3.4 TWR and input estimation 12

4 Passive control 13
4.1 Controllability-lacking test rigs 14
4.2 Cost functions 19

5 Summaries of appended papers 20

6 Concluding remarks and future work 21

References 21

II Appended Papers A–E 29

Part I
Extended Summary

1 Introduction and motivation

An important aspect of laboratory testing within the field of structural dynamics is input control. When assessing structural integrity under dynamic loads, dynamic fatigue, rattle and squeak, or structure-borne vibrations, how to make sure that the load- and vibration levels are comparable to the ones which the tested product will experience in the span of its lifetime? For a long time, one of the testing engineer's most trusted tools has been to use measurements from older product life history, or early-version products submitted to working conditions, as a reference signal for dynamic testing, replicated by use of linear iterations in the frequency domain. This method is known as Time Waveform Replication.

One of the first examples of the Time Waveform Replication (TWR) algorithm applied to structural dynamics testing was presented by Cryer et. al. [9]. The paper describes an attempt at replicating measured wheel accelerations by inverting the frequency domain transfer function from vertical load input at the wheel thread to acceleration output at the wheel spindle. While this direct method proved unsuccessful, it was found that by approaching the solution iteratively (compensating for modeling errors and nonlinearities), good agreement between measured output and desired response could be achieved.

Such early efforts have been followed by many others, to the point that TWR has been included in the US military testing standard [87] as well as commercial testing software, *e.g.* [37]. While initially being used on systems with (next to) collocated sensors and actuators, developments to account for more sensors than actuators [12, 50] have enticed study of which sensor outputs to replicate in order to achieve the best correlation with an end goal [96], in the specific study cited induced fatigue damage.

These developments combine to imply another question of importance: If the input of the TWR algorithm is not collocated with the output to be tracked, the set of controllable and that of observable modes of the test specimen may differ. Furthermore, if all load transfer paths that were activated during the acquisition of the reference signal cannot be replicated in the testing facilities, one might face the situation that there is an observable contribution to the reference signal which is uncontrollable from the test rig input. This may lead to unrealistic loading and poor tracking. Such controllability shortcomings have been reported in literature in the case of component testing, where the intuitive solution to alter the input configuration was utilized to somewhat counter the effects [11].

But what if that is not possible? Many test rigs are composed of large shakers, frequently hydraulic, rigidly mounted to ground. If controllability should be lacking in such a test setup, the approach to alter the input configuration is not applicable. So what to do then? This thesis aims at investigating an approach using passive control components, inspired by the use of semi-passive control in energy-optimal control of multi-body systems [81].

Paper B - D use a Finite Element (FE) model to design such a passive control component. In **Paper B** and **Paper C**, the methodology of passive control component design based on high-fidelity FE models is developed in the context of optimization. **Paper B** describes a two-step gradient-based optimization procedure to design the passive component. This approach is however cumbersome and likely hard to implement on larger-scale problems, wherefore an approach using a global search method (Genetic Algorithms) was argued in **Paper C**. In **Paper D**, the method was validated using laboratory testing of a simple structure. For the implementation of such an approach, it is vital that the FE model used for the design of the passive control component is of high quality. To this end, model calibration, previously known as model updating, is needed. This is the subject of **Paper A**. An alternative approach to passive control components design, sidestepping the need for a validated FE model by use of substructure synthesis, was developed in **Paper E**.

2 Models in structural dynamics

System descriptions in structural dynamics can be separated into *external* and *internal* descriptions. In an internal description, the dynamics of the system is described by some internal *states*, whereas an external description offers information on the input- output relation without internal variables, (*c.f.* [5, 46]). Moreover, an internal description is typically realization-dependent. The principal difference between internal and external descriptions is shown schematically in figures 2.1 and 2.2, where the former shows an external and the latter an internal model structure. This chapter deals exclusively with linear models.

2.1 External description

For a typical structural dynamics system modeled in continuous time, which is passive and time-invariant, an external description in the time domain is given by the convolution relation:

$$\mathbf{y}(t) = \int_{-\infty}^{\infty} \mathbf{g}(t-\tau)\mathbf{u}(\tau)d\tau \tag{2.1}$$

Assuming that the *impulse response* $\mathbf{g}(t)$ is an analytical function, the system can equivalently be described in terms of the *Markov parameters* of the system, defined in the continuous-time case as the coefficients of a Taylor expansion of $\mathbf{g}(t)$ [5, 46].

In practice, real dynamic systems are often sampled at discrete time instances because of the need for digital signal processing. A similar expression as (2.1) holds for discrete time, but replacing the convolution integral by a convolution sum. In discrete time, the argument t is often used as the integer sample number rather than time, such that sampled

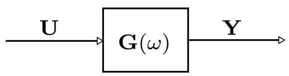

Figure 2.1: *External model structure. The dynamics of the system is represented by a "black box" - here exemplified by a frequency-domain transfer function.*

time instants t_s relate to t by the sampling interval Δ_t as $t_s = \Delta_t t$. For discrete external models, the Markov parameters are defined by the shift operator applied to $\mathbf{g}$ such that $\mathbf{g}_k = \mathbf{g}(t-k)$. Markov parameters of casual discrete-time systems are often structured in a specific block matrix form which is constant along the anti-diagonals known as a Hankel matrix, $\mathcal{H}$ *cf.* [5, 46]:

$$\mathcal{H} = \begin{bmatrix} \mathbf{g}_1 & \mathbf{g}_2 & \cdots & \mathbf{g}_k & \mathbf{g}_{k+1} & \cdots \\ \mathbf{g}_2 & \mathbf{g}_3 & \cdots & \mathbf{g}_{k+1} & \mathbf{g}_{k+2} & \cdots \\ \vdots & \vdots & ⋰ & \vdots & \vdots & ⋰ \\ \mathbf{g}_k & \mathbf{g}_{k+1} & \cdots & \mathbf{g}_{2k-1} & \mathbf{g}_{2k} & \cdots \\ \mathbf{g}_{k+1} & \mathbf{g}_{k+2} & \cdots & \mathbf{g}_{2k} & \mathbf{g}_{2k+1} & \cdots \\ \vdots & \vdots & ⋰ & \vdots & \vdots & \end{bmatrix} \tag{2.2}$$

Note that $\mathbf{g}_0$ is not included; thus, an outer description of a causal discrete-time system is given by the instantaneous action defined by $\mathbf{g}_0$ and the dynamic action defined by $\mathcal{H}$ [5]. Descriptions of this type are important for the realization problem, discussed in the next section.

By applying Laplace transform to equation (2.1), the convolution expression reduces to multiplication [5, 85]:

$$\mathbf{Y}(s) = \mathbf{G}(s)\mathbf{U}(s) \tag{2.3}$$

Where $\mathbf{G}(s)$ is the Laplace transform of the impulse response $\mathbf{g}(t)$, known as the transfer function of the system. In structural dynamics, systems are often subject to periodic excitation, $\mathbf{u}(t) = \mathbf{U}(\omega)e^{i\omega t}$. Evaluating the transfer function over the imaginary axis, that is, by letting the complex argument s of (2.3) satisfy $s = i\omega$, where $\omega \in \mathcal{R}$, the *Frequency Response Function* (FRF) matrix is acquired[1]:

$$\mathbf{Y}(\omega) = \mathbf{G}(\omega)\mathbf{U}(\omega) \tag{2.4}$$

Here, the imaginary unit $i = \sqrt{-1}$ has been dropped in the argument for convenient notation. The relation is also shown in figure 2.1. It represents the value of a system output by a stationary harmonic unit excitation at a given input and frequency:

$$G_{jk}(\omega) = \frac{Y_j(\omega)}{U_k(\omega)} \tag{2.5}$$

In other words: The response of the system at output k to harmonic excitation at input j with frequency ω is a harmonic function with the same frequency, whose magnitude has been amplified by a factor $|G_{jk}(i\omega)|$ and phase shifted by $\angle G_{jk}(i\omega)$ (*cf.* [85]). Similar relations hold for discrete-time systems, using instead discrete Laplace/Fourier transforms.

Structural dynamics testing for identification of models results in outer models of the structure, most frequently FRF matrices. Depending on whether the output consists of accelerations, velocities or displacements, the FRF matrix is alternatively termed *accelerance*, *mobility* or *receptance* matrix, respectively. Modal testing is thoroughly described in textbooks, *e.g.* by Ewins [21].

[1]In which case the Laplace transform can be viewed as the real-valued Fourier transform [22].

2.2 Internal description

Internal is an epithet assigned to models in which the time evolution of the dynamical system is described by a differential equation on some internal state, along with algebraic equations to map the state to the model output. In structural dynamics, many computational models are derived using first principles, such as Newton's laws, and a proper discretization of the problem, resulting in the second-order equation:

$$\mathbf{M}\ddot{\mathbf{q}}(t) + \mathbf{V}\dot{\mathbf{q}}(t) + \mathbf{K}\mathbf{q}(t) = \mathbf{f}(t) \tag{2.6}$$

Here, $\mathbf{M}$ is the mass matrix, $\mathbf{V}$ is the viscous damping matrix and $\mathbf{K}$ is the stiffness matrix, while the vectors $\mathbf{q}(t)$ and $\mathbf{f}(t)$ are the displacement and force vectors, respectively (*cf.* [27]). A dot denotes differentiation with respect to time. Thus, the internal state of this model is the displacement of the system. In many cases, the calculated displacements are also the sought-after output of the system; the implicit output equation is then $\mathbf{y}(t) = \mathbf{I}\mathbf{q}(t)$, where $\mathbf{I}$ is the appropriately sized identity matrix.

The second order problem of equation (2.6) can be rewritten into a linear first-order form. Such models are popular in several engineering fields and are referred to as *state-space* models, depicted as in figure 2.2 (see further [64], [85]):

$$\begin{aligned} \dot{\mathbf{x}}(t) &= \mathbf{A}\mathbf{x}(t) + \mathbf{B}\mathbf{u}(t) \\ \mathbf{y}(t) &= \mathbf{C}\mathbf{x}(t) + \mathbf{D}\mathbf{u}(t) \end{aligned} \tag{2.7}$$

Here, $\mathbf{A}$, $\mathbf{B}$, $\mathbf{C}$ and $\mathbf{D}$ are known as the state-, input-, output- and direct throughput matrix, respectively. $\mathbf{x}(t)$ is the state vector, $\mathbf{u}(t)$ the input vector and $\mathbf{y}(t)$ the output vector. Furthermore, the first equation of (2.7) is sometimes called the state equation, making the second the output equation. Assuming that $\mathbf{M}$ is invertible, a way to transfer the second-order equation (2.6) to a first-order state equation form is to define the matrices as [64]:

$$\mathbf{A} = -\begin{bmatrix} \mathbf{0} & -\mathbf{I} \\ \mathbf{M}^{-1}\mathbf{K} & \mathbf{M}^{-1}\mathbf{V} \end{bmatrix} \quad \mathbf{B} = \begin{bmatrix} \mathbf{0} \\ \mathbf{M}^{-1} \end{bmatrix} \mathbf{P}_i \tag{2.8}$$

Where $\mathbf{P}_i$ is the distribution matrix for input, that is, $\mathbf{f}(t) = \mathbf{P}_i\mathbf{u}(t)$.

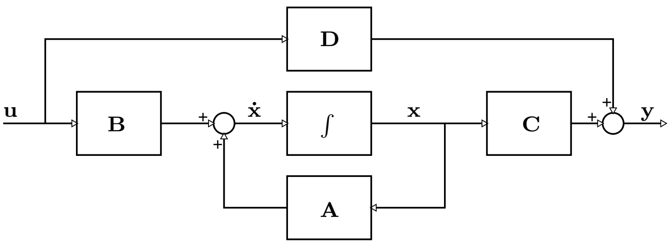

Figure 2.2: *Internal model structure. The dynamics of the system is represented by the evolution of the internal state, governed by some differential equation. An internal model is here exemplified by a first-order state space model.*

The *dynamic stiffness matrix* $\mathbf{Z}(\omega)$ of a system is established assuming periodicity, such that the time dependence of the system response can be reduced to a harmonic multiplier:

$$\mathbf{Z}(\omega)\mathbf{Q}(\omega)e^{i\omega t} = \left(-\omega^2\mathbf{M} + i\omega\mathbf{V} + \mathbf{K}\right)\mathbf{Q}(\omega)e^{i\omega t} = \mathbf{F}(\omega)e^{i\omega t} \tag{2.9}$$

From equation (2.9), it is evident that the inverse of the dynamic stiffness matrix is equivalent to the frequency response according to the definition in equation (2.4) when the system output is the displacement vector $\mathbf{Q}(\omega)$ and its input the force vector $\mathbf{F}(\omega)$. This serves to illustrate that an external description is easily calculated from an internal.

The reverse however is not true. The problem of developing an inner model from an outer is referred to as the realization problem [5]. FRF and Markov parameter representations are the inputs to modal parameter estimation techniques [6, 45, 38] and system identification procedures [57, 62] for developing internal models.

The popular modal parameter estimation technique known as the Eigensystem Realization Algorithm (ERA) [38] identifies a state-space system with zero throughput from the Hankel matrix (2.2) by use of singular value decomposition, from which modal parameters are extracted and presented to the user. The system identification methods known as state-space subspace system identification (4sid) techniques also use the Markov parameters [57]. *E.g.* in [62], two frequency domain versions of 4sid are described, the first of which utilize a similar singular value decomposition of a Hankel matrix as ERA, acquired from Inverse Discrete Fourier Transform (IDFT), for estimation of $\mathbf{A}$ and $\mathbf{C}$ in (2.7), but identifying $\mathbf{B}$ and $\mathbf{D}$ from a linear least squares problem in a second step.

System identification results in a model of the form in (2.7). In this thesis, frequency-domain state-space subspace system identification, by the `n4sid` function in matlab, is used to estimate modal parameters from the eigensolution of the identified $\mathbf{A}$ matrix in **paper A** and **paper D**. Assume that a state-space realization $\{\mathbf{A}, \mathbf{B}, \mathbf{C}, \mathbf{D}\}$ has been found. Its frequency-domain transfer function is then:

$$\mathbf{G}(\omega) = \mathbf{C}\left((i\omega)\mathbf{I} - \mathbf{A}\right)^{-1}\mathbf{B} + \mathbf{D} \tag{2.10}$$

Letting $\mathbf{T}$ be an invertible matrix of the appropriate size, it is easy to verify that the system $\{\mathbf{T}^{-1}\mathbf{AT}, \mathbf{T}^{-1}\mathbf{B}, \mathbf{CT}, \mathbf{D}\}$ will have the same transfer function; hence, internal models are not unique: Any transformation of this kind, known as a *similarity transform*, will yield the same outer model and thus the same input-output relation, but another set of system matrices as above, and a different state vector, $\boldsymbol{\xi} = \mathbf{T}^{-1}\mathbf{x}$. The most widely used similarity transform is perhaps the diagonalizing transform, which transforms the system such that the internal description consists of system eigenvalues and generalized eigenvectors. Such a transformation is hence also used in ERA [38].

2.3 Parametric model calibration

Model validation and model calibration[2] is important whenever results from computational models are used for design. Aspects of model calibration is the topic of **paper A**, and model calibration and validation is applied in **paper D**. An overview of some of the aspects of validation and calibration is given here. See also [23, 61].

There is a subtle difference between modal parameter estimation/system identification and parametric model calibration: In identification, an internal model with low rank to define the input-output relation defined by a test is sought, whereas in a corresponding parametric model calibration, a parameterized high-order model is calibrated such that its input-output relation matches the measured in the desired frequency domain. Hence, identification techniques may be used to characterize the measurements, so that the compared quantities are eigenvalues and/or eigenvectors instead.

The calibration and validation process is begun by acquisition of a set of reference test data from a series of vibrational tests in laboratory, typically consisting of either frequency response functions or eigenvalues and eigenvectors. Parts of this reference data set is then compared to results from a corresponding calculation on the computational model to be validated; if the discrepancy is low enough, the model is said to have been *validated* with respect to measured data. If not, the parametric model (2.11) needs to be *calibrated* with respect to the measured data.

$$\mathbf{M}(\mathbf{p})\ddot{\mathbf{q}}(t) + \mathbf{V}(\mathbf{p})\dot{\mathbf{q}}(t) + \mathbf{K}(\mathbf{p})\mathbf{q}(t) = \mathbf{f}(t) \tag{2.11}$$

Here, $\mathbf{p} \in \mathbf{P}$ refers to the parameters describing the model and their admissible set, respectively. Thus, a key feature in model validation and calibration is the metric used for comparing measured and analytical results. This metric may differ between the validation and calibration stages. Given a vectorial quantity of comparison $\Delta\mathbf{q}$, defined as the difference between analytical and experimental quantities such that $\Delta\mathbf{v} = \mathbf{v}_{FEM} - \mathbf{v}_{measured}$, validation with respect to symmetrical deviations of the metric can be expressed as:

$$-\boldsymbol{\sigma} < \Delta\mathbf{v} < \boldsymbol{\sigma} \tag{2.12}$$

Where $\boldsymbol{\sigma}$ is some tolerance level vector. Similarly, parametric model calibration can be described mathematically as the optimization problem:

$$\mathbf{p}^{\star} = \arg\min_{\mathbf{p}\in\mathbf{P}} \|\Delta\mathbf{v}\| \tag{2.13}$$

Conventionally, the norm $\|\cdot\|$ used is the sum of squares, but that is not a prerequisite unless using a dedicated optimization method. In this thesis, the term *error metric* is used for $\Delta\mathbf{v}$, whether used for calibration or validation.

The choice of parametrization is also crucial in parametric model calibration. The topic is discussed in the influential book by Friswell and Mottershead [23], describing in

[2] also known as *model updating* - a term lately used more frequently to describe the process in which models are updated as a result of new *specifications* in the product development process, as opposed to the calibration of model parameters to ensure correlation with performed dynamic tests. In this thesis, it is however used as a synonym to model calibration. The terms will be used interchangeably.

particular the Best Subspace Method by Lallement and Piranda [53]. Another example of parameter discrimination techniques is the Orthogonality Co-linearity Index by Linderholt and Abrahamsson [56, 55]. Using experience from a number of experiments, Mottershead *et al.* [65] furthermore argued that finite element models are most prone to errors in structural joints and that distances and angles of such joints are most suitable as parameters for calibration. Friswell, Mottershead and Ahmadian [24] also argue geometrical parameters over stiffness and mass parameters.

Several comparative studies have been published advocating one error metric over another for use in model calibration, *e.g.* [30, 52]. Friswell and Mottershead [23] describe many of the error metrics still considered in the field. Historically, the question of which type of data to use in model calibration has been subject to much debate: Many papers have been written advocating the use of modal data in the calibration procedure, such as [1, 20, 29, 80, 52, 92]; as much has been written on using FRF data more or less directly [7, 31, 36, 35, 51, 54]. Some also advocate the use of transmission zeros, or antiresonances, along with eigenfrequencies [10, 44, 66].

Recent applications of model calibration reported in literature include calibration of models for the ARES I-X pathfinder vehicle, using principal component analysis of FRFs to construct an error metric and including also analysis of variance (ANOVA) considerations [34], and the Berke arch dam, using eigenvalues extracted from operational modal analysis [82].

3 Time Waveform Replication

The Time Waveform Replication algorithm is an iterative method to calculate the input needed to track a desired output. It works on frequency domain data. In control terms, it can be described as a linear Iterative Learning Control (ILC) algorithm. In the PhD thesis by Dijkstra [17], it is proposed that ILC can be interpreted as both a feed-forward and a feedback algorithm; the process of ILC is a block-feedback process, while the signal from the off-line feedback is implemented as feed-forward, that is, during each iteration, there is no feedback control. In algebraic terms, the algorithm reads:

$$\mathbf{U}_{n+1}(\omega_k) = \mathbf{U}_n(\omega_k) + \mathbf{Q}\bar{\mathbf{G}}^{+}(\omega_k)\left(\mathbf{R}(\omega_k) - \mathbf{Y}_n(\omega_k)\right) \tag{3.1}$$

Here, $\mathbf{R}(\omega_k)$ is the frequency domain reference signal, the discrete fourier transform of a measured time-domain reference signal $\mathbf{r}(t_k)$. Likewise, $\mathbf{Y}_n(\omega_k)$ is the frequency domain response to load $\mathbf{U}_n(\omega_k)$. Hence $\mathbf{Y}_n(\omega_k)$ is acquired by transforming $\mathbf{U}_n(\omega_k)$ to the time domain by the inverse discrete Fourier transform and a digital-to-analog converter (DAC), and applying the resulting continuous-time signal to the test specimen through the shakers while recording samples of the output from the test specimen in $\mathbf{y}(t_k)$, which is then transformed to the frequency domain. $\mathbf{Q}$ is a safety factor matrix to prevent overcompensation and ensure convergence. Finally, $\bar{\mathbf{G}}^{+}(\omega_k)$ is the pseudoinverse of the estimated transfer function, acquired by structural dynamic identification testing, *cf.* section 2.1.

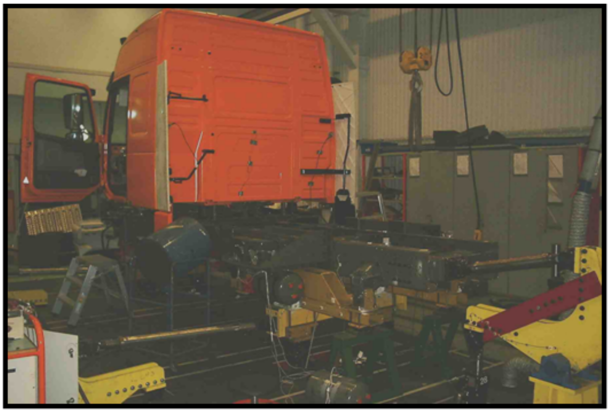

Figure 3.1: *Example of TWR application in industry. Durability testing of truck cab at Volvo Group Trucks Technology testing facilities.*

3.1 TWR in industry

As previously stated, the TWR algorithm (or augmentations of it) is frequently used in industry to estimate the required input for tracking of a desired output sequence. Its most frequent users are found in the road vehicle industries; in the Gothenburg area, these are represented by companies such as the Volvo Group. Volvo Group Trucks Technology perform durability tests on trucks and truck components, see figure 3.1; their procedure for such tests is:

- An instrumented vehicle is driven several laps at the test track at Hällered. Several test drivers may be employed to account for differences in drive styles.
- An experienced test engineer inspects the time-domain data collected and selects parts of the recorded time history to be replicated in the test rig based on severity. This data set is used for reference in the test.
- A transfer function for the rig and test specimen setup is acquired through random excitation at the expected input levels of the test. Transfer functions at several load levels might be used and compared.
- An estimate of the inverse transfer function is calculated by SVD-based pseudo-inversion of the identified transfer function.
- TWR iterations to replicate the reference signal are commenced, using commercial software from rig manufacturer. During iterations, weighting functions of different frequency bands as well as different channels may be set. These can be varied during the test.
- The iterations proceed until the test engineer is content that the reference is replicated satisfactorily.

- Actual durability test is run, where the calculated input signal is applied to the test specimen numerous times. Fatigue life predictions are based on the number of iterations until failure, mapped by the relation to test track laps. This is in turn related to an expected life length under ordinary working conditions.

3.2 Contraction mapping and convergence

Assume that there are i inputs, j outputs and k frequency points of a given TWR test procedure. Let the input function u_n, consisting of the input $\mathbf{U}_n(\omega_k)$ at every frequency point ω_k of the algorithm in equation (3.1), be defined as an element of the general complex *input space* $\mathcal{C}^{ik}$ such that:

$$u_n = \left[\begin{array}{cccc} \mathbf{U}_n^T(\omega_1) & \cdots & \mathbf{U}_n^T(\omega_k) & \cdots \end{array} \right]^T \tag{3.2}$$

Define the elements of the complex *output space* $\mathcal{C}^{jk}$ similarly:

$$y_n = \left[\begin{array}{cccc} \mathbf{Y}_n^T(\omega_1) & \cdots & \mathbf{Y}_n^T(\omega_k) & \cdots \end{array} \right]^T \tag{3.3}$$

It is obvious that the linear relation (2.4) is defined by letting G be an element of $\mathcal{C}^{jk \times ik}$. Furthermore, G will then be a block diagonal matrix. Hence, this enlarged definition ensures that all linear systems are represented by linear maps $\mathcal{C}^{ik} \to \mathcal{C}^{jk}$. The definition also allows for certain properties associated with nonlinear systems, notably coupling between different frequencies, to be allowed in the context of linear mappings.

To asses the algorithmic convergence in a noise-free setting, define the unknown real system as the possibly nonlinear mapping G from the input space to the output space:

$$G : \mathcal{C}^{ik} \to \mathcal{C}^{jk} \tag{3.4}$$

Let $Q\bar{G}^+$ be a linear mapping from from $\mathcal{C}^{jk}$ to $\mathcal{C}^{ik}$. The TWR algorithm described in equation (3.1) can then be written as:

$$u_{n+1} = u_n + Q\bar{G}^+(r - y_n) \tag{3.5}$$

$$y_n = Gu_n \tag{3.6}$$

Where $r, y_n \in \mathcal{C}^{jk}\ \forall n$ and $u_n \in \mathcal{C}^{ik}\ \forall n$. Thus, the evolution of the input sequence can be written as:

$$u_{n+1} = Q\bar{G}^+ r + (I - Q\bar{G}^+ G)u_n \tag{3.7}$$

By defining the mappings T and $\tilde{T}$ as:

$$T : \mathcal{C}^{ik} \to \mathcal{C}^{ik} \quad : u = Tx = x - Q\bar{G}^+ Gx \tag{3.8}$$

$$\tilde{T} : \mathcal{C}^{ik} \to \mathcal{C}^{ik} \quad : u = \tilde{T}x = Q\bar{G}^+ r + Tx \tag{3.9}$$

It is evident that the input evolution of equation (3.7) can be written as $u_{n+1} = \tilde{T}u_n$. By Banach's fixed point theorem [15, 93], $\tilde{T}$ has a unique fixed point u_∞ such that $u_\infty = \tilde{T}u_\infty$ if it is a contraction, *i.e.* if:

$$\|\tilde{T}x - \tilde{T}y\| \leq c\|x - y\| \quad , \quad 0 < c < 1 \quad \forall x, y \in \mathcal{C}^{ik} \tag{3.10}$$

Which, by the definitions of equations (3.8) and (3.9), can be rewritten as:

$$\|\tilde{T}x - \tilde{T}y\| = \|Q\bar{G}^{+}r + Tx - (Q\bar{G}^{+}r + Ty)\| = \\ \|Tx - Ty\| \leq c\|x - y\| \tag{3.11}$$

For a general nonlinear system G, this is as far as the contraction mapping approach will take us. Equation (3.11) defines the condition for $\tilde{T}$ to be a contraction, ensuring global convergence of the TWR algorithm. Assuming however that we are in a linear range, so that the mapping G can be assumed linear in the generalized sense discussed above, T will also be a linear mapping. We may then use the result:

$$\|Tx - Ty\| = \|T(x - y)\| \leq \|T\|\|x - y\| \tag{3.12}$$

And hence, $\tilde{T}$ is a contraction if $\|T\| < 1$, that is, if:

$$\|T\| = \|I - Q\bar{G}^{+}G\| < 1 \tag{3.13}$$

Essentially, this means that the TWR algorithm converges, for linear systems, if $\bar{G}^{+}$ is an adequate approximation of the inverse of G. Furthermore, it shows that a poor inverse model can be compensated to some extent by a small Q. This is in line with the experiences from using the algorithm, *e.g.* [9].

If T, and thereby $\tilde{T}$, is a contraction, it defines a linear convergence, as from (3.11), we have that (see further [93]):

$$\|u_{\infty} - u_n\| \leq \frac{c^n}{1 - c}\|Tu_0 - u_0\| \tag{3.14}$$

Where u_0 is the starting point of the iterations and u_{∞} is the fixed point. Furthermore, if $\tilde{T}$ is a contraction, we have from (3.7) and the definition of a fixed point, *i.e.* $\tilde{T}u_{\infty} = u_{\infty}$ that:

$$u_{\infty} = Q\bar{G}^{+}r + u_{\infty} - Q\bar{G}^{+}Gu_{\infty} \\ \Rightarrow Q\bar{G}^{+}r - Q\bar{G}^{+}Gu_{\infty} = 0 \tag{3.15}$$

If we define the output corresponding to the input-space fixed point as $y_{\infty} = Gu_{\infty}$ from equation (3.6), we furthermore have that:

$$Q\bar{G}^{+}(r - y_{\infty}) = 0 \tag{3.16}$$

This final result holds as long as u_{∞} is a fixed point of $\tilde{T}$, that is, without the assumption that $\tilde{T}$ is a global contraction. It assures that in the absence of noise, the projection of the output error by $Q\bar{G}^{+}$ will be minimized. Such convergence also motivates the use of TWR iterations in virtual testing, as discussed in [58]. Further convergence studies, including noise *etc.*, can be found in the PhD theses by Markusson [60] and de Cuyper [12].

3.3 Drive signal generation methods

The TWR method is historically the most widely used drive signal generation method in dynamic testing. In recent years, a lot of contributions to the drive signal generation problem have been reported in literature. Plummer [73] gives a good overview in a paper on control applications for structural dynamics testing. The objectives of research in drive signal generation have been to decrease time until convergence while increasing or maintaining tracking accuracy. To this end, a research group in Belgium proposed an augmentation of the TWR algorithm to encompass online feedback. In [14], the concept is discussed and evaluated on a single input single output (SISO) test rig, while in *e g* [4, 90, 91] multiple input multiple output (MIMO) applications are concerned. It is argued that while the design of a robust MIMO feedback controller (*e g* using μ-synthesis) is difficult, adopting a decoupling transformation can simplify the controller design while still improving both convergence rate and accuracy. This decoupling process was the focus of some research in turn [89].

Similarly, decoupling was also concerned by Koch *et al.* in the design of a four poster electrodynamic direct body excitation rig [48, 49, 50]. In ordinarily TWR-controlled test rigs, typically using hydraulic actuators, it is sufficient to control each actuator by an off-the shelf controller such as a PID; the TWR iterations will ensure convergence even though this might be sub-optimal [74, 73]. The need for online MIMO control in the work by Koch *et al.*, in place of the more conventional decentralized (PID) control, was due to inherent instability and strong inter-actuator coupling in the electrodynamic actuators, used in place of conventional hydraulic actuators. However, the TWR algorithm is conventionally applied to the closed-loop system, while in the work by the Belgian group referred to above, TWR was applied to the open-loop system (in turn consisting of closed control loops over each actuator, equipped with industrial standard controllers) and enhanced by feedback in an outer loop. Plummer [73] refers to the latter as "closing-the-loop on the remote parameters".

In an earlier paper, Plummer [74] noted that due to the iterative nature of drive signal generation common in industry, non-optimal closed-loop control is often tolerated, and proceeded to argue that the iterative approach is sometimes not applicable, notably when the specimen is severely damaged by the first iteration, *e g* in earthquake testing. Therefore, a modal control algorithm, essentially decoupling the dynamics to diagonal modal form, is implemented for a shaker table and shows improved tracking.

It should be noted that in controlling a shaker table, the structure is essentially rigid with unknown unbalance and, possibly, dynamic disturbance due to the test piece resting on top of it. Since several shakers are connected through the table top, it is harder than controlling individual shakers, but likely not as hard as controlling an unknown, fully dynamical, MIMO structure. Thus, the intended application should be kept in mind when considering and comparing different control strategies.

In place of a decoupling procedure, Gizatullin and Edge [28] used an augmented decentralized adaptive minimal control synthesis (MCS) with four adaptive gains, augmented by an inverse model feed-forward term and a PID controller to control a shaker table. This type of adaptive control is referred to by Plummer [73] as direct, as the controller gains are adapted directly. The other type of adaptive control applies a filter to the reference/command signal, and is known as Adaptive Inverse Control (AIC) [73, 95]. Shen *et al.* [83] combined both approaches for a shaker table controller, using adaptive MCS and AIC with an autoregressive moving average model with exogeneous inputs (ARMAX) structure. In a related study, Shen *et al.* [84] used instead a simpler finite impulse response (FIR) pre-filter AIC to adapt an off-line identified feed-forward inverse model to specimen damage for earthquake testing. A decentralized FIR filter AIC approach has also been commercialized for MIMO test rigs, with in addition information passed between shakers [88]. See also results in [67].

The involved shaker-table controllers of the preceding paragraph share the appealing property that, if an iterative approach is necessary, next iteration input can be calculated on-line. For (hydraulic) test rigs, Raath [75] suggested a time-domain iteration procedure based on system identification of an auto-regressive model with exogenous inputs, which was reset into discrete-time state-space form, to be able to calculate next iteration input online (with delay) by implicit inversion. The method was evaluated on a collocated hydraulic four-poster test rig setup for a pickup truck. Using state-space subspace system identification and Stable Dynamic Inversion (see [25, 26]) was applied with some success to a SISO tracking problem by DeCuyper and Verhaegen [13]. It was also augmented to include feedback as in [14].

3.4 TWR and input estimation

The drive signal generation methods can be coarsely distinguished into groups by the load identification, or input estimation, method mimicked: The classical TWR approach uses frequency domain inversion [50], while in the time-domain approaches adaptive filters [88], and state-space model inversion [75, 13] is used, respectively, whereas the modal control [74] is related to modal load identification. In studies by Allen and Carne [2, 3] and Nordström and Nordberg [71], different load identification procedures are compared. The first study relates two similar time-domain methods, essentially filter approaches with delay calculated by pseudo-inverting a Toeplitz matrix representation of truncated Markov parameters, derived in a setting similar to the Stable Dynamic Inversion approach [13] and named Inverse Structural Filter (ISF), to a modal and a frequency domain inversion load identification technique. The second relates ISF, a modal, a wavelet and a least-squares approach. Allen and Carne found that the original ISF is highly sensitive to the choice of delay, and therefore proposed an augmentation allowing multiple delays by enriching a state space representation in a manner similar to the "inverting the input-output map" system inversion approach [26], yielding results comparable with frequency-domain inversion. Nordström and Nordberg found that ISF and the least-squares approach dubbed Dynamic Programming were good. In a follow-up study [72], the non-minimum phase problem reported for ISF was addressed by allowing individual time delays for each measurement channel. See also [68, 69].

Nordström went on working on the least squares approach, eventually devising an independently time-discretized general minimization formulation allowing nonlinear model structures, solved in a Lagrangian setting by Newton iterations [70] (implemented by Ronasi *et al.* [79] as well). Such a general optimization framework was also presented by

Markusson *et al.* [59] in an article on Iterative Learning Control. As described previously, TWR is a linear form of ILC; Markusson *et al.* thus show that it can be viewed as a special case of Newton iteration. This was also recognized by Hay and Roberts [33, 76], who used this generalization to device an augmentation of the classical TWR approach for nonlinear applications, specifically for test rig tracking. ILC for nonlinear test rig tracking has also been studied by Smolders *et al.* [86].

It is important to note that drive signal generation methods share traits with input estimation techniques, as the purpose of TWR is typically interpreted to be the accurate reproduction of the loads, or inputs, which excited the system during the reference measurement. This paradigm was shifted, at least for squeak and rattle (S&R), by a number of papers advocating the use of direct body excitation over classical forcing at the wheelbase during S&R analysis, primarily due to the relative silence of electromagnetic shakers compared to electrohydraulic shakers [8, 48, 49, 50]. Such an approach implicitly targets some objective, to which the outputs to be tracked must be sensitive, rather than the accurate estimation of some unknown input. A somewhat similar philosophy for durability testing can be traced in the paper by Xu *et al.* [96], where the induced fatigue damage from tests in which the drive signal has been calculated based on different outputs is compared in terms of damage induced, by the Palmgren-Miner linear fatigue criterion. Such a comparison could however likely be fit in to the input estimation framework as well.

The TWR approach in itself can actually be seen as a step towards indirect reproduction of the component's working conditions; another testing paradigm of vehicle testing insists the input to be road surface roughness data [18, 19, 47, 77, 78, 94], controlling the shaker input according to some statistical model of roughness and travel speed. As the measured reference signal is bound to contain vibratory components caused by engine and wind loading, the input pattern of a TWR run is likely to differ from such an approach.

4 Passive control

Passive vibration control is well known in the field of structural dynamics, where the term is commonly applied to the problem of reducing unwanted vibration through structural modification [63]. The most commonly encountered passive vibration control component is perhaps the tuned mass damper (also known as a dynamic absorber or vibration neutralizer), which essentially enforces a vibrational node at a desired frequency and point of a given structure, thereby reducing vibration levels (*cf.* [16]).

The approach pursued in this thesis shares many traits with such systems; however, instead of reducing unwanted vibrations, the goal is here to allow the system to accurately track a reference signal which was previously unattainable due to vibrational nodes at the input position of the system. In essence, the end result sought is hence the antithesis of that of classical vibration control; we aim to move vibrational nodes *away* from an excitation point of a given structure.

In this sense, the passive control of this thesis is more closely related to semi-passively actuated multibody systems. In a manner similar to that presented here, Berbyuk [81] showed that a combination of active control and passive (spring) and/or semi-passive

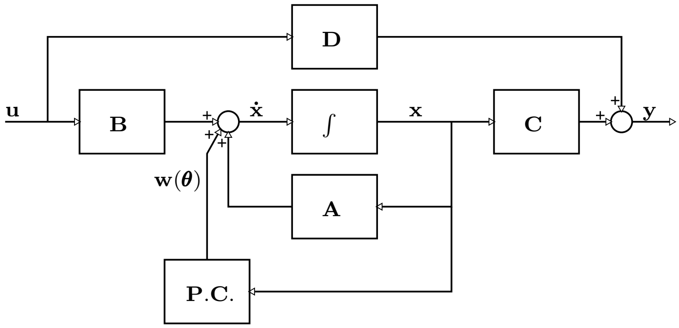

Figure 4.1: *Example of passive control concept: Linear system on state-space form modified by a passive control component. By adjusting the system boundaries, such a passive component can be viewed as a structural modification.*

elements required lower actuation energy compared to using only active control approaches only for energy-optimal control problems such as bipedal locomotion systems.

The main theme of the work presented in this thesis concerns the design of passive control components to improve tracking properties in dynamic test rigs lacking controllability whose input configurations cannot be altered. A conceptual explanation of the idea is given in figure 4.1 for a linear system. As is seen, the introduction of the passive system will alter the transfer function from the active input to the output; hence, it may be viewed as a structural modification. It is intuitively obvious that such an approach will affect the controllability properties of the system.

When using this perspective, it is important to remember that the structure under study is, in fact, still the same; only its boundary conditions have been altered. Furthermore; the situation we attempt to remedy using such passive components is such that the reference signal contains contributions from modes which are uncontrollable in the test rig. That the reference signal contains such contributions is an indication that the boundary conditions of the rig were off from the start, or that all load paths of the real world have not been accounted for in the laboratory. This is a very likely scenario; any vehicle driven on test track would experience vibrations due to engine and wind loading as well as road excitation. A classical four-poster test (*e.g.* [90]), with vertical loading at each wheel of a car, could certainly be inadequate in case, say, engine loading contributed significantly to the measured target response at the test track.

4.1 Controllability-lacking test rigs

An important contribution towards the understanding of the effects of controllability shortcomings in dynamic test rigs is given in the appendix of **paper C**. The main result shows that under certain conditions, it is impossible to minimize the output error of a controllability-lacking test rig, and under other, the input levels required to minimize the output error will be large. Furthermore, while not mutually exclusive, at least one of the conditions will be met if the reference signal contains contributions from well-separated modes that are uncontrollable in the test rig.

The results in **paper C** are derived assuming that the direct throughput of the tested system is zero. For structural dynamics models, this is true when displacement and velocity outputs are considered, but not necessarily so for acceleration outputs. As the sensors used in structural dynamics testing often measure acceleration, a version of the proof for acceleration output is given here.

Begin with a general linear time-invariant state-space model with velocity output, and hence zero direct throughput, *i e*:

$$\begin{aligned} \dot{\mathbf{x}}(t) &= \mathbf{A}\mathbf{x}(t) + \mathbf{B}\mathbf{u}(t) \\ \mathbf{y}_\mathbf{v}(t) &= \mathbf{C}_\mathbf{v}\mathbf{x}(t) \end{aligned} \tag{4.1}$$

As $\{\mathbf{A}, \mathbf{B}, \mathbf{C}_\mathbf{v}, \mathbf{0}\}$ is linear and time-invariant by assumption, a model with acceleration output can be acquired since $\mathbf{y}_\mathbf{a}(t) = \dot{\mathbf{y}}_\mathbf{v}(t) = \mathbf{C}_\mathbf{v}\dot{\mathbf{x}}(t)$ and $\dot{\mathbf{x}}(t)$ is related to $\mathbf{x}(t)$ and $\mathbf{u}(t)$ by the state equation in (4.1) as:

$$\begin{aligned} \dot{\mathbf{x}}(t) &= \mathbf{A}\mathbf{x}(t) + \mathbf{B}\mathbf{u}(t) \\ \mathbf{y}_\mathbf{a}(t) &= \mathbf{C}_\mathbf{v}\mathbf{A}\mathbf{x}(t) + \mathbf{C}_\mathbf{v}\mathbf{B}\mathbf{u}(t) \end{aligned} \tag{4.2}$$

Let us assume that the eigenvalues of $\mathbf{A}$ are separated and let $\mathbf{\Phi}$ and $\mathbf{\Lambda}$ be the eigensolution to $\mathbf{A}$, satisfying $\mathbf{A\Phi} = \mathbf{\Phi\Lambda}$, where $\mathbf{\Phi}$ is the matrix whose columns are the eigenvectors and $\mathbf{\Lambda}$ is a diagonal matrix of eigenvalues; let $\mathbf{x}(t) = \mathbf{\Phi}\boldsymbol{\eta}(t)$. This similarity transform yields:

$$\begin{aligned} \dot{\boldsymbol{\eta}}(t) &= \mathbf{\Lambda}\boldsymbol{\eta}(t) + \mathbf{\Phi}^{-1}\mathbf{B}\mathbf{u}(t) \\ \mathbf{y}_\mathbf{a}(t) &= \mathbf{C}_\mathbf{v}\mathbf{A}\mathbf{\Phi}\boldsymbol{\eta}(t) + \mathbf{C}_\mathbf{v}\mathbf{B}\mathbf{u}(t) \end{aligned} \tag{4.3}$$

By applying the Laplace transform and noting that $\mathbf{A\Phi} = \mathbf{\Phi\Lambda}$, this becomes:

$$\begin{aligned} s\mathbf{H}(s) &= \mathbf{\Lambda}\mathbf{H}(s) + \mathbf{\Phi}^{-1}\mathbf{B}\mathbf{U}(s) \\ \mathbf{Y}_\mathbf{a}(s) &= \mathbf{C}_\mathbf{v}\mathbf{\Phi}\mathbf{\Lambda}\mathbf{H}(s) + \mathbf{C}_\mathbf{v}\mathbf{B}\mathbf{U}(s) \end{aligned} \tag{4.4}$$

Since the left eigenvector matrix is the inverse of the right, such that $\mathbf{\Phi}^{-1} = \mathbf{\Psi}^H$, where $(\cdot)^H$ denotes Hermitian transpose, the transfer function $\mathbf{G}(s)$ is:

$$\mathbf{Y}_\mathbf{a}(s) = \mathbf{G}(s)\mathbf{U}(s) = \mathbf{C}_\mathbf{v}\left(\mathbf{\Phi\Lambda}\left(s\mathbf{I} - \mathbf{\Lambda}\right)^{-1}\mathbf{\Psi}^H + \mathbf{I}\right)\mathbf{B}\mathbf{U}(s) \tag{4.5}$$

By the assumption that the eigenvalues are separated, the first term of the transfer function can be rewritten as:

$$\begin{bmatrix} \cdots & \mathbf{C}_\mathbf{v}\boldsymbol{\phi}_i & \cdots \end{bmatrix} \begin{bmatrix} \ddots & & \\ & \frac{\lambda_i}{s-\lambda_i} & \\ & & \ddots \end{bmatrix} \begin{bmatrix} \vdots \\ \boldsymbol{\psi}_i^H\mathbf{B} \\ \vdots \end{bmatrix} = \sum_{i=1}^{N} \frac{\lambda_i}{s-\lambda_i}\mathbf{C}_\mathbf{v}\boldsymbol{\phi}_i\boldsymbol{\psi}_i^H\mathbf{B} \tag{4.6}$$

The PBH eigenvector test for controllability [46] states that if $\boldsymbol{\psi}_i^H\mathbf{B} \neq \mathbf{0}$ for all i, the system is state controllable, and conversely, if some state satisfies the corresponding equality, the system is not state controllable. ($\mathbf{C}\boldsymbol{\phi}_i \neq \mathbf{0}$ is the test for state observability.)

This definition additionally makes it possible to identify the uncontrollable state(s). Consider a case where a reference signal $\mathbf{R}(s)$ has been retrieved by applying the unknown input signal $\tilde{\mathbf{U}}(s)$ to the acceleration-output system $\{\mathbf{A}, \tilde{\mathbf{B}}, \mathbf{C_v A}, \mathbf{C_v}\tilde{\mathbf{B}}\}$, which is to be replicated by the system $\{\mathbf{A}, \mathbf{B}, \mathbf{C_v A}, \mathbf{C_v B}\}$. The only difference between these systems is hence $\mathbf{B}$ contra $\tilde{\mathbf{B}}$, corresponding to a change of input configuration. By (4.5) and (4.6), we have that:

$$\mathbf{R}(s) = \sum_{i=1}^{N} \frac{\lambda_i}{s-\lambda_i} \mathbf{C_v} \boldsymbol{\phi}_i \boldsymbol{\psi}_i^H \tilde{\mathbf{B}}\tilde{\mathbf{U}}(s) + \mathbf{C_v}\tilde{\mathbf{B}}\tilde{\mathbf{U}}(s) \tag{4.7}$$

$$\mathbf{Y}(s) = \sum_{i=1}^{N} \frac{\lambda_i}{s-\lambda_i} \mathbf{C_v} \boldsymbol{\phi}_i \boldsymbol{\psi}_i^H \mathbf{B}\mathbf{U}(s) + \mathbf{C_v}\mathbf{B}\mathbf{U}(s) \tag{4.8}$$

And the error function in the Laplace domain can be defined as:

$$\begin{aligned}\mathbf{E}(s) =& \mathbf{R}(s) - \mathbf{Y}(s) \\ =& \sum_{i=1}^{N} \mathbf{C_v}\boldsymbol{\phi}_i \left(\frac{\lambda_i}{s-\lambda_i} \boldsymbol{\psi}_i^H \tilde{\mathbf{B}}\tilde{\mathbf{U}}(s) - \frac{\lambda_i}{s-\lambda_i} \boldsymbol{\psi}_i^H \mathbf{B}\mathbf{U}(s) \right) \ldots \\ & + \mathbf{C_v}\tilde{\mathbf{B}}\tilde{\mathbf{U}}(s) - \mathbf{C_v}\mathbf{B}\mathbf{U}(s) \end{aligned} \tag{4.9}$$

Since $\boldsymbol{\psi}_i^H$ is a $1 \times N$ vector, $\mathbf{B}$ an $N \times n_{\text{in}}$ array and $\mathbf{U}(s)$ an $n_{\text{in}} \times 1$ vector, the terms $\boldsymbol{\psi}_i^H \tilde{\mathbf{B}}\tilde{\mathbf{U}}(s)$ and $\boldsymbol{\psi}_i^H \mathbf{B}\mathbf{U}(s)$ are scalar quantities. Let $a_i(s) = \boldsymbol{\psi}_i^H \tilde{\mathbf{B}}\tilde{\mathbf{U}}(s)$ and $b_i(s) = \boldsymbol{\psi}_i^H \mathbf{B}\mathbf{U}(s)$. Furthermore, denote the output eigenvectors $\boldsymbol{\phi}_{Ci} = \mathbf{C_v}\boldsymbol{\phi}_i$. The error in (4.9) can then be simplified to:

$$\mathbf{E}(s) = \sum_{i=1}^{N} \boldsymbol{\phi}_{Ci} \frac{\lambda_i \left(a_i(s) - b_i(s)\right)}{s-\lambda_i} + \mathbf{C_v}\tilde{\mathbf{B}}\tilde{\mathbf{U}}(s) - \mathbf{C_v}\mathbf{B}\mathbf{U}(s) \tag{4.10}$$

Assume now, without lack of generality, that one state is uncontrollable in the system $\{\mathbf{A}, \mathbf{B}, \mathbf{C_v A}, \mathbf{C_v B}\}$. By the PBH eigenvector test for controllability, this corresponds to a situation where $\boldsymbol{\psi}_k^H \mathbf{B} = \mathbf{0}$, and hence $b_k(s) = 0$. Furthermore, note that $\mathbf{B}\mathbf{U}(s)$ and $\tilde{\mathbf{B}}\mathbf{U}(s)$ are vectors in $\mathcal{C}^N$. Since $\boldsymbol{\Phi}$ is an invertible matrix, its N columns $\boldsymbol{\phi}_i$ are linearly independent, and thus form a basis of $\mathcal{C}^N$ (over the field of complex numbers). Expressing $\mathbf{B}\mathbf{U}(s)$ and $\tilde{\mathbf{B}}\mathbf{U}(s)$ in this basis yields:

$$\tilde{\mathbf{B}}\mathbf{U}(s) = \sum_{i=1}^{N} c_i(s)\boldsymbol{\phi}_i \tag{4.11}$$

$$\mathbf{B}\mathbf{U}(s) = \sum_{i=1}^{N} d_i(s)\boldsymbol{\phi}_i \tag{4.12}$$

However, regardless of input $\mathbf{U}(s)$ the condition $\boldsymbol{\psi}_k^H \mathbf{B}\mathbf{U}(s) = 0$ holds for all s as $\boldsymbol{\psi}_k^H \mathbf{B} = \mathbf{0}$. Furthermore, $\boldsymbol{\psi}_k^H \boldsymbol{\phi}_i = \delta_{ki}$, where δ_{ki} equals one if $k = i$ and zero otherwise. Thus, we can write the PBH condition above in the eigenvector basis as:

$$0 = \boldsymbol{\psi}_k^H \mathbf{B}\mathbf{U}(s) = \sum_{i=1}^{N} d_i(s) \boldsymbol{\psi}_k^H \boldsymbol{\phi}_i = \sum_{i=1}^{N} d_i(s)\delta_{ki} = d_k(s) \tag{4.13}$$

Thus, the error of equation (4.10) can be written as:

$$\mathbf{E}(s) = \sum_{i\neq k}^{N} \boldsymbol{\phi}_{Ci} \left(\frac{\lambda_i(a_i(s) - b_i(s))}{s - \lambda_i} + c_i(s) - d_i(s) \right) + \boldsymbol{\phi}_{Ck} \left(\frac{\lambda_k a_k(s)}{s - \lambda_k} + c_k(s) \right) \tag{4.14}$$

Denote the space spanned by $\{\boldsymbol{\phi}_{Ci}\}_{i\neq k}$ with S, such that $S = \text{span}\{\boldsymbol{\phi}_{Ci}\}_{i\neq k} \subset C^N$. Its orthogonal complement is $S^\perp$. The uncontrollable state can then be decomposed such that:[1]

$$\boldsymbol{\phi}_{Ck} = \boldsymbol{\phi}_{Ck}^{S} + \boldsymbol{\phi}_{Ck}^{S^\perp} \tag{4.15}$$

Where $\boldsymbol{\phi}_{Ck}^{S} \in S$ and $\boldsymbol{\phi}_{Ck}^{S^\perp} \in S^\perp$. Since the first term is in the space spanned by $\{\boldsymbol{\phi}_{Ci}\}_{i\neq k}$, it can be written as a linear combination of these vectors, and the error can be rewritten again as:

$$\begin{aligned}
\mathbf{E}(s) =& \sum_{i\neq k}^{N} \boldsymbol{\phi}_{Ci} \left(\frac{\lambda_i(a_i(s) - b_i(s))}{s - \lambda_i} + c_i(s) - d_i(s) \right) + \left(\boldsymbol{\phi}_{Ck}^{S} + \boldsymbol{\phi}_{Ck}^{S^\perp} \right) \left(\frac{\lambda_k a_k(s)}{s - \lambda_k} + c_k(s) \right) \\
=& \sum_{i\neq k}^{N} \boldsymbol{\phi}_{Ci} \left(\frac{\lambda_i(a_i(s) - b_i(s))}{s - \lambda_i} + c_i(s) - d_i(s) + \alpha_i \left(\frac{\lambda_k a_k(s)}{s - \lambda_k} + c_k(s) \right) \right) \quad \cdots \\
& + \boldsymbol{\phi}_{Ck}^{S^\perp} \left(\frac{\lambda_k a_k(s)}{s - \lambda_k} + c_k(s) \right) = \mathbf{E}_S(s) + \mathbf{E}_{S^\perp}(s)
\end{aligned} \tag{4.16}$$

Clearly, the two error terms belong in the respective spaces indicated. By looking at the square of the complex modulus of the error function and using the fact that vectors in S and $S^\perp$ are orthogonal by definition, it is found that:

$$\begin{aligned}
|\mathbf{E}(s)|^2 &= |\mathbf{E}_S(s) + \mathbf{E}_{S^\perp}(s)|^2 \\
&= |\mathbf{E}_S(s)|^2 + \mathbf{E}_S^H(s)\mathbf{E}_{S^\perp}(s) + \mathbf{E}_{S^\perp}^H(s)\mathbf{E}_S(s) + |\mathbf{E}_{S^\perp}(s)|^2 \\
&= |\mathbf{E}_S(s)|^2 + |\mathbf{E}_{S^\perp}(s)|^2 \geq |\mathbf{E}_{S^\perp}(s)|^2
\end{aligned} \tag{4.17}$$

Posing a lower bound on the error function whenever the output eigenvector of the uncontrollable state is linearly independent from the others. This is at least the case for the JimBeam example studied in this thesis, verified by the results in **paper C-E**.

If the vectors $\{\boldsymbol{\phi}_{Ci}\}_{i\neq k}$ are linearly dependent, the decomposition of $\boldsymbol{\phi}_{Ck}^{S}$ is not unique. This is the case whenever the number of outputs is less than the number of controllable states, or when one or more state is unobservable. Let therefore $\{\mathbf{e}_j\} \in S$ be an orthonormal basis of S, such that $\boldsymbol{\phi}_{Ci} = \sum_j \beta_{ij}\mathbf{e}_j$ and $\boldsymbol{\phi}_{Ck}^{S} = \sum_j \gamma_j \mathbf{e}_j$. Clearly, these decompositions are unique. Recall also from (4.12) and (4.13) that $\sum_{i\neq k} \boldsymbol{\phi}_{Ci} d_i(s) = \mathbf{C_v B U}(s)$. Expressing this in the basis $\{\mathbf{e}_j\}$ instead, so that $\mathbf{C_v B U}(s) = \sum_j \mathbf{e}_j \hat{d}_j(s)$,

[1]Note that the implication of the result in (4.13), used to set up (4.14), is that $\mathbf{C_v B U}(s) \in S$. Hence, only elements in S can be excited in the test rig.

where $\hat{d}_j(s) = \mathbf{e}_j^H \mathbf{C_v} \mathbf{B} \mathbf{U}(s)$ by the projection formula, the error in S can be written as:

$$\begin{aligned}
\mathbf{E}_S(s) =& \sum_{i \neq k} \left(\sum_j \beta_{ij} \mathbf{e}_j \right) \left(\frac{\lambda_i (a_i(s) - b_i(s))}{s - \lambda_i} + c_i(s) \right) \quad \dots \\
& + \sum_j \gamma_j \left(\frac{\lambda_k a_k(s)}{s - \lambda_k} + c_k(s) \right) \mathbf{e}_j + \mathbf{C_v} \mathbf{B} \mathbf{U}(s) \\
=& \sum_j \left(\sum_{i \neq k} \beta_{ij} \left(\frac{\lambda_i (a_i(s) - b_i(s))}{s - \lambda_i} + c_i(s) \right) \quad \dots \right. \\
& \left. + \hat{d}_j(s) + \gamma_j \left(\frac{\lambda_k a_k(s)}{s - \lambda_k} + c_k(s) \right) \right) \mathbf{e}_j
\end{aligned} \tag{4.18}$$

Since the basis vectors are orthogonal, they are linearly independent. For (4.18) to be zero it is therefore necessary that the following holds for all j:

$$\sum_{i \neq k} \beta_{ij} \frac{\lambda_i b_i(s)}{s - \lambda_i} + \hat{d}_j(s) = \sum_{i \neq k} \beta_{ij} \left(\frac{\lambda_i a_i(s)}{s - \lambda_i} + c_i(s) \right) + \gamma_j \left(\frac{\lambda_k a_k(s)}{s - \lambda_k} + c_k(s) \right) \tag{4.19}$$

Now, all dependance on the control force is on the left hand side; since $b_i(s) = \boldsymbol{\psi}_i^H \mathbf{B} \mathbf{U}(s)$ and $\hat{d}_j(s) = \mathbf{e}_j^H \mathbf{C_v} \mathbf{B} \mathbf{U}(s)$:

$$\begin{aligned}
\sum_{i \neq k} \beta_{ij} \frac{\lambda_i b_i(s)}{s - \lambda_i} + \hat{d}_j(s) &= \sum_{i \neq k} \beta_{ij} \frac{\lambda_i}{s - \lambda_i} \boldsymbol{\psi}_i^H \mathbf{B} \mathbf{U}(s) + \mathbf{e}_j^H \mathbf{C_v} \mathbf{B} \mathbf{U}(s) \\
&= \left(\sum_{i \neq k} \beta_{ij} \frac{\lambda_i}{s - \lambda_i} \boldsymbol{\psi}_i^H + \mathbf{e}_j^H \mathbf{C_v} \right) \mathbf{B} \mathbf{U}(s)
\end{aligned} \tag{4.20}$$

On the right hand side of (4.19), let $f(s) = \sum_{i \neq k} \beta_{ij} \left(\frac{\lambda_i a_i(s)}{s - \lambda_i} + c_i(s) \right) + \gamma_j c_k(s)$. Then:

$$\begin{aligned}
\left| f(s) + \gamma_j \frac{\lambda_k a_k(s)}{s - \lambda_k} \right| &= \left| \left(\sum_{i \neq k} \beta_{ij} \frac{\lambda_i}{s - \lambda_i} \boldsymbol{\psi}_i^H + \mathbf{e}_j^H \mathbf{C_v} \right) \mathbf{B} \mathbf{U}(s) \right| \\
&\leq \left| \sum_{i \neq k} \beta_{ij} \frac{\lambda_i}{s - \lambda_i} \boldsymbol{\psi}_i^H \mathbf{B} + \mathbf{e}_j^H \mathbf{C_v} \mathbf{B} \right| |\mathbf{U}(s)|
\end{aligned} \tag{4.21}$$

$$\Rightarrow \qquad \frac{\left| f(s) + \gamma_j \frac{\lambda_k a_k(s)}{s - \lambda_k} \right|}{\left| \sum_{i \neq k} \beta_{ij} \frac{\lambda_i}{s - \lambda_i} \boldsymbol{\psi}_i^H \mathbf{B} + \mathbf{e}_j^H \mathbf{C_v} \mathbf{B} \right|} \leq |\mathbf{U}(s)| \tag{4.22}$$

For a lightly damped mechanical system, when $s = j\omega$ is close to the pole λ_k, the second numerator term of (4.22) will become very large. Since no term inverse-proportional to

$s - \lambda_k$ exists in the denominator, the control force will have to be large as well in order to remove $\mathbf{E}_S(s)$ and hence minimize $\mathbf{E}(s)$. This is also confirmed in the numerical results of **paper B-C**.

4.2 Cost functions

In this thesis, passive control components are designed in an optimization framework. In essence, this framework consists of a model M_s of the controllability-lacking structure, a parameterized model of the intended passive component $M_p(\theta_p)$ depending on some parameters θ_p, a (possibly) parameterized process $\mathcal{G}(M_s, M_p, \theta_c)$ for coupling the two models such that $M_{sp}(\theta_p, \theta_c) = \mathcal{G}(M_s, M_p(\theta_p), \theta_c)$ and a cost function $J(M_{sp}(\theta_p, \theta_c))$. The final component of the framework is a solver for the problem:

$$\min_{\{\theta_p, \theta_c\} \in \Theta} J(M_{sp}(\theta_p, \theta_c)) \tag{4.23}$$

From **paper B** through **paper E**, an evolution of modeling, coupling and solution methods for the optimization problem of passive components design is described and motivated. The cost functions used however subtly change as well.

A first effort, which ended up as a preliminary step in the elaborate optimization solver for passive components design described in **paper B**, used a continuous controllability metric by Hamdan and Nayfeh [32] in maximizing the controllability of the least controllable mode. While making the system controllable, it did not yield a system optimal for tracking a desired reference signal (which can be seen when comparing the cost function contour plots of **paper B**), so it was discarded with the gradient-based optimization method in favor of off-the-shelf global search methods in **paper C-D**.

The remaining cost functions all consist of some scalar quantity of the output error and the input force calculated from the coupled model $M_{sp}(\theta_p, \theta_c)$. Thus, these cost functions consist of two terms with different units; in **paper B**, they are weighted together as the classical optimization approach pursued in that paper warrants a scalar cost function. Later, a Pareto-optimality approach was used. This allows the practicing engineer to make the engineering judgement of the relative importance once results are known rather than in advance, which is likely to appeal. In **paper B-D** the quantities compared are the norms of frequency domain signals, *i.e.* $\|\mathbf{E}\|$ and $\|\mathbf{U}\|$, where the first term is the output error; the 2-norm was used for this term. For the second, input term, the maximum, or ∞-norm was used as a measure of the highest force levels was sought.

In **paper E**, this is pursued in a more direct manner, by calculating the inverse Fourier transform of the input signal, so that the measure is actually the expected highest force level, $\|\mathcal{F}^{-1}(\mathbf{U})\|_\infty$. Moreover, the output error term is modified slightly to allow it to be interpreted as the RMS value of the error in the time domain through Parceval's theorem. While the second change is likely cosmetic, the first one represents a change with respect to previous papers. The motivation for the change was that it is better to use whichever criterion is limiting for the force in the calculations in order to be able to make useful predictions, and that the largest value in the frequency domain does not necessarily correlate to the time domain. The approach is however not applicable (at least not in the same straightforward manner) for the approach where a validated Finite

Element model is used to set up the model M_s, as in **paper B-D**, since in these papers the frequency resolution was decreased in the calculations as compared to the testing for computational efficiency.

To conclude this section: Ultimately, the choice of exact cost function formulation in designing a passive component for improved tracking in a given test rig should be governed by the aim of the experiment to be performed. Since the work of this thesis has been aimed at developing a method for designing such passive components only (the testing has focused on recreating a given output only, not on investigating, say, fatigue properties of some test specimen), the exact formulation of cost functions has been deliberately vague. Using some measure of the input magnitude $\|\mathbf{U}\|$ to complement a measure of the output error $\|\mathbf{E}\|$ is however likely to be fruitful, as the results of **paper B** and **paper E** suggest the existence of regions in the parameter spaces where high input is required to little effect in $\|\mathbf{E}\|$.

5 Summaries of appended papers

In **paper A**, *Comparison of several error metrics for FE model updating*, error metrics used for model updating, or calibration, are compared using a simple spring-mass structure from the literature as benchmark. The error metrics are compared with respect to three equally weighted criteria: 1) The smoothness and convexity of the associated cost function, evaluated by ocular inspection of cost function plots. 2) The identifiability of the parameter space, evaluated by the condition number of an approximate Hessian. 3) The performance of the error metrics in the presence of noise, evaluated by the inverse of the Fisher information matrix through the Cramer-Rao lower bound.

In **paper B**, *Increased controllability in component testing using structural modifications*, the concept of using passive components for improving the tracking abilities of dynamic test rigs is introduced and a method for designing such passive components in an optimization framework is developed. The method relies on a Finite Element model of the tested system. The design problem is solved in two steps: In the first step, the passive component is designed in such a way that the controllability of the least controllable mode is maximized. In the second, the actual reference signal to be tracked is used, and virtual experiments are conducted to set up a cost function consisting of the calculated output tracking error and the input levels. The method is verified on a simple numerical example.

In **paper C**, *A method for improving test rig performance using passive components*, the passive components approach is investigated further, and the design method of **paper B** is discarded in favor of off-the-shelf Genetic Algorithms applied to a multi-objective formulation of the second step cost function of **paper B** in order for a more straightforward application of the methodology. A more elaborate numerical example is used to further verify the passive components approach. Included as an appendix to the paper is a theoretical motivation for the passive components approach, which shows that if states that are not controllable in the test rig contribute to the reference signal, the required input signal may be large and/or the output error not fully removed.

In **Paper D**, *Application of passive components for improved tracking in controllability-lacking test rigs*, the methodology of **paper C** is verified in an experimental study of a simple structure consisting of three plates joint by bolts. A validated Finite Element model of the structure is acquired through model calibration using techniques discussed in **paper A**. A phenomenological approach to the modeling of joints is used for the parametrization. The validated model is used for designing a passive component, which is manufactured and attached to the structure. The experimental results presented show that the output error has decreased by 50% by the use of the passive control system.

In **Paper E**, *An experimental approach to improve controllability in test rigs using passive components*, an approach for designing passive components without having to resort to a Finite Element model is introduced. It relies on system identification to model the system under study experimentally and couples it to a passive component model using experimental-analytical dynamic substructuring. While in the experimental validation performed in the paper measurements from the test rig setup alone is shown to be sufficient for accurate-enough identification of the experimental system model, it is acknowledged that in most cases, additional modal testing could be needed. The parametrization in this paper differs from that of **paper B-D** in that the attachment point of the passive component can only be chosen at a pre-defined subset of measured candidate positions.

6 Concluding remarks and future work

This thesis is concerned with such dynamic testing as aims at the accurate reproduction of a pre-defined reference signal. It has been shown that when there are well-separated modes included in such reference signals which the test rig is not able to reproduce, *i.e.* when there is a lack of controllability in the test setup, the control force required for tracking and/or the tracking error will be large.

A concept of passive control to improve the tracking properties of dynamic test rigs suffering from lack of controllability for which the input configuration cannot be altered has been developed. Two distinct methods, one relying on high quality Finite Element modeling and the other on experimental modeling of the structure to be tested, have been developed. The validity of the concept, and the two methods, has been verified in small-scale tests.

Furthermore, techniques for automated model updating, or calibration, have been investigated. A methodology for comparing different updating formulations has been introduced and model updating has been successfully applied to a real structure.

Regarding the concept of passive control, a theoretical framework for its implementation has been developed. A lot of work still needs to be done before the methodology can be said to be fruitful, most notably tests on real-life structures such as a road vehicle. The use of reduction methods in the design method by Finite Element models should be thoroughly investigated, and further investigations into the effects on end goals, such as fatigue life predictions, should be performed.

References

[1] T. Abrahamsson, M. Andersson, and T. McKelvey. “A Finite Element Model Updating Formulation Using Frequency Responses and Eigenfrequencies”. *NAFEMS 2nd International Conference on Structural Dynamics Modelling*. 1997.

[2] M. S. Allen and T. G. Carne. “Comparison of Inverse Structural Filter (ISF) and Sum of Weighted Accelerations Technique (SWAT) time domain force identification methods”. *47th AIAA-ASME-ASCE-AHS-ASC Structures, Structural Dynamics, and Materials Conference*. 2006.

[3] M. S. Allen and T. G. Carne. Delayed, multi-step inverse structural filter for robust force identification. *Mechanical Systems and Signal Processing* **22** (2008), 1036–1054.

[4] J Anthonis et al. Feedback Approach for Reproduction of Field Measurements on a Hydraulic Four Poster. *Biosystems Engineering* **96** (2007), 435–445.

[5] A. C. Antoulas. *Approximation of large-scale dynamical systems.* Advances in design and control. Society for Industrial and Applied Mathematics, SIAM, 2005. ISBN: 978-0-898716-58-0.

[6] P Avitabile. *TUTORIAL NOTES: Structural Dynamics and Experimental Modal Analysis.* Modal Analysis and Controls Laboratory, University of Massachusetts, Lowell, MA. 2000.

[7] C. Bolsman. “FE model updating using measured FRF’s”. MA thesis. Technische Universiteit Delft, 2005.

[8] R. S. Brines, L. G. Weiss, and E. L. Peterson. The Application of Direct Body Excitation Toward Developing a Full Vehicle Objective Squeak and Rattle Metric. *SAE Technical Paper 2001-01-1554, doi:10.4271/2001-01-1554* (2001).

[9] B. W. Cryer, P. E. Nawrocki, and R. A. Lund. *Road simulation system for heavy duty vehicles.* SAE paper 760361. 1976.

[10] W. D’Ambrogio and A. Fregolent. Results obtained by minimising natural frequency and antiresonance errors of a beam model. *Mechanical Systems and Signal Processing* **17**.1 (2003), 29–37.

[11] F De Coninck et al. “Durability Assessment of Lightweight Stainless Steel Exhaust Systems”. *ISMA 2008 Conference on Noise and Vibration Engineering*. 2008.

[12] J de Cuyper. “Linear Feedback Control for Durability Test Rigs in the Automotive Industry”. PhD thesis. Katholieke Universiteit Leuven, 2006. ISBN: 90-5682-688-3.

[13] J De Cuyper and M Verhaegen. State Space Modeling and Stable Dynamic Inversion for Trajectory Tracking on an Industrial Seat Test Rig. *Journal of Vibration and Control* **8** (2002), 1033–1050.

[14] J de Cuyper, M Verhaegen, and J Swevers. Off-line feed-forward and $\mathcal{H}_\infty$ feedback control on a vibration rig. *Control Engineering Practice* **11** (2003), 129–140.

[15] L Debnath and P Mikusiński. *Introduction to Hilbert Spaces with Applications.* 3rd edition. London: Elsevier Academic, 2005. ISBN: 0-12-208438-1.

[16] J. P. den Hartog. *Mechanical Vibrations.* 3rd edition. McGraw-Hill Book Company, Inc., New York, 1947.

[17] B. G. Dijkstra. “Iterative Learning Control, with applications to a wafer stage”. PhD thesis. Delft University of Technology, 2004.
[18] C. J. Dodds and J. D. Robson. Simulation of Dynamic Stresses in Vehicles and Components. *Vehicle System Dynamics* **4** (1975), 130–134.
[19] C. J. Dodds and J. D. Robson. The Description of Road Surface Roughness. *Journal of Sound and Vibration* **31** (1973), 175–183.
[20] B. Ebeling. “FE-Modell-Korrektur anhand modaler Meßdaten”. MA thesis. Technische Universität Hamburg-Harburg, 2003.
[21] D. J. Ewins. *Modal testing: theory practice and application.* 2nd edition. Baldock: Research Studies Press, 2000.
[22] G. B. Folland. *Fourier analysis and its applications.* Pacific Groove, California: Wadswirth & Brooks/Cole Advanced Books & Software, 1992.
[23] M. I. Friswell and J. E. Mottershead. *Finite element model updating in structural dynamics.* Vol. 38. Solid Mechanics and its Applications. Kluwer Academic Publishers, 1995.
[24] M. I. Friswell, J. E. Mottershead, and H. Ahmadian. Finite-element model updating using experimental test data: parametrization and regularization. *Philosophical Transactions of the Royal Society A* **359** (2001), 169–186.
[25] K. George. “Input Estimation Techniques for Robust Output Tracking”. *Proceedings of the International Conference on Advances in Control and Optimization.* 2007, pp. 309–316.
[26] K. George and M. Verhaegen. “Stable Inversion of MIMO Linear Discrete Time Non-Minimum Phase Systems”. *Proceedings of the 7th Mediterranean Conference on Control and Automation (MED99).* 1999, pp. 267–281.
[27] M Geradin and D Rixen. *Mechanical vibrations: theory and application to structural dynamics.* 2nd edition. John Wiley and sons ltd, 1995.
[28] A. O. Gizatullin and K. A. Edge. Adaptive control for a multi-axis hydraulic test rig. *Proceedings of the Institution of Mechanical Engineers Part I - Journal of Systems and Control Engineering* **221** (2007), 183–198.
[29] D. Göge. Automatic updating of large aircraft models using experimental data from ground vibration testing. *Aerospace Science and Technology* **7** (2003), 33–45.
[30] D. Göge and M. Link. Assessment of computational model updating procedures with regard to model validation. *Aerospace Science and Technology* **7** (2003), 47–61.
[31] H. Grafe. “Model Updating of Large Structural Dynamics Models Using Measured Response Functions”. PhD thesis. University of London, 1998.
[32] A. M. A. Hamdan and A. H. Nayfeh. Measures of Modal Controllability and Observability for First- and Second-Order Linear Systems. *Journal of guidance, control, and dynamics* **12**.3 (1989), 421–428.
[33] N. C. Hay and D. E. Roberts. Iterative control in automotive testing. *Proceedings of the Institution of Mechanical Engineers, Part I: Journal of Systems and Control Engineering* **221** (2007), 223–233.
[34] L. G. Horta et al. “Finite Element Model Calibration Approach for Ares I-X”. *Structural Dynamics, Volume 3.* Ed. by T. Proulx. Vol. 12. Conference Proceedings of the Society for Experimental Mechanics Series. Springer New York, 2011, pp. 1037–1054.

[35] M Imregun, K. Y. Sanliturk, and D. J. Ewins. Finite element model updating using frequency response function data II. Case study on a medium-size finite element model. *Mechanical Systems and Signal Processing* **9** (1995), 203–213.
[36] M Imregun, W. J. Visser, and D. J. Ewins. Finite element model updating using frequency response function data I. Theory and initial investigation. *Mechanical Systems and Signal Processing* **9** (1995), 187–202.
[37] Instron Structural Testing Systems. *RS TWR - A module of RS LabSite*. Product information sheet. 2004.
[38] R. S. P. J-N Juang. An eigensystem realization algorithm for modal parameter identification and model reduction. *Journal of Guidance, Control, and Dynamics* **8** (1985), 620–627.
[39] A. T. Johansson and T. J. S. Abrahamsson. *A method for improving test rig performance using passive components*. Submitted for international publication. 2012.
[40] A. T. Johansson and T. J. S. Abrahamsson. "An experimental approach to improve controllability in test rigs using passive components". *Submitted to ISMA 2012 the International Conference on Noise and Vibration Engineering*. 2012.
[41] A. T. Johansson and T. J. S. Abrahamsson. *Application of passive components for improved tracking in controllability-lacking test rigs*. Submitted for international publication. 2012.
[42] A. T. Johansson and T. J. S. Abrahamsson. "Increased controllability in component testing using structural modifications". *Proceedings of ISMA 2008 the International Conference on Noise and Vibration Engineering*. 2008.
[43] A. T. Johansson, T. J. S. Abrahamsson, and F van Keulen. "Comparison of several error metrics for FE model updating". *Proceedings of IMAC XXV, the International Modal Analysis Conference*. 2007.
[44] K Jones and J Turcotte. Finite element model updating using antiresonant frequencies. *Journal of Sound and Vibration* **252**.4 (2002), 717–727.
[45] R. R. C. Jr and A. J. Kurdila. *Fundamentals of Structural Dynamics*. Hoboken, New Jersey: John Wiley & Sons, 2006. ISBN: 0-471-43044-7.
[46] T Kailath. *Linear Systems*. Englewood Cliffs, New Jersey: Prentice-Hall, 1980.
[47] D.-K. Kang, S.-H. Lee, and S.-H. Goo. Development of Standardization and Management System for the Severity of Unpaved Test Courses. *Sensors* **7** (2007), 2004–2027.
[48] U Koch, D Wiedemann, and H Ulbrich. "Decoupled decentral control of electromagnetic actuators for car vibration excitation". *Proceedings of the 2009 IEEE Conference on Mechatronics*. 2009.
[49] U Koch et al. "State-space modelling and decoupling control of electromagnetic actuators for car vibration excitation". *Proceedings of the 2009 IEEE Conference on Mechatronics*. 2009.
[50] U. Koch, D. Wiedemann, and H. Ulbrich. Model-Based MIMO State-Space Control of a Car Vibration Test Rig With Four Electromagnetic Actuators for the Tracking of Road Measurements. *IEEE Transactions on Industrial Electronics* **58** (2011), 5319–5323.

[51] K.-S. Kwon and R.-M. Lin. Frequency selection method for FRF-based model updating. *Journal of Sound and Vibration* **278**.1-2 (2004), 285–306.
[52] K.-S. Kwon and R.-M. Lin. Robust finite element model updating using Taguchi method. *Journal of Sound and Vibration* **280** (2005), 77–99.
[53] G Lallement and J Piranda. "Localization Methods for Parametric Updating of Finite Elements Models in Elastodynamics". *8th International Modal Analysis Conference*. 1990.
[54] R. M. Lin and D. J. Ewins. Analytical model improvement using frequency response functions. *Mechanical Systems and Signal Processing* **8**.4 (1994), 437–458.
[55] A. Linderholt and T. Abrahamsson. Optimising the informativeness of test data used for computational model updating. *Mechanical Systems and Signal Processing* **18** (2005), 736–750.
[56] A. Linderholt and T. Abrahamsson. Parameter identifiability in finite element model error localisation. *Mechanical Systems and Signal Processing* **17**.3 (2003), 579–588.
[57] L Ljung. *System Identification: Theory for the user*. 2nd edition. Englewood Cliffs, New Jersey: Prentice Hall, 1999.
[58] LMS International. *BMW - Using Virtual Test Rigs for Loads Prediction*. URL: http://www.lmsintl.com/BMW-virtual-test-rigs-load-prediction, downloaded 131111. 2011.
[59] O Markusson, H Hjalmarsson, and M Norrlöf. "A General Framework for Iterative Learning Control". *Proceedings of the 15th IFAC World Congress*. 2002.
[60] O. Markusson. "Model and System Inversion with Applications in Nonlinear System Identification and Control". PhD thesis. Royal Institute of Technology, 2002. ISBN: 91-7283-228-2.
[61] R. L. Mayes. "Model correlation and calibration". *Proceedings of the 27th International Modal Analysis Conference, Orlando, FL*. 2009.
[62] T. McKelvey, H. Akcay, and L. Ljung. Subspace-based multivariable system identification from frequency response data. *Automatic Control, IEEE Transactions on* **41** (1996), 960 –979.
[63] D. Mead. *Passive vibration control*. John Wiley & Sons Ltd, Chichester, England, 1999. ISBN: 9780471942030.
[64] L Meirovitch. *Dynamics and Control of Structures*. New York: Wiley-Interscience, 1990. ISBN: 0-471-62858-1.
[65] J. E. Mottershead et al. Geometric Parameters for finite element model updating of joints and constraints. *Mechanical Systems and Signal Processing* **10**.2 (1996), 171–182.
[66] D. Nam et al. Improved parameter identification using additional spectral information. *International Journal of Solids and Structures* **42**.18-19 (5), 4971–4987.
[67] K. S. Narendra and N. O. Oleng. Exact Output Tracking in Decentralized Adaptive Control Systems. *IEEE Transactions on Automatic Control* **47** (2002), 390–395.
[68] T. P. Nordberg. "Time Domain Methods for Load Identification of Linear and Nonlinear Systems". PhD thesis. Chalmers University of Technology, 2004. ISBN: 91-7291-489-0.
[69] L. J. Nordström. "Input Estimation in Structural Dynamics". PhD thesis. Chalmers University of Technology, 2005. ISBN: 91-7291-668-0.

[70] L. J. L. Nordström, H Johansson, and F Larsson. A Strategy for Input Estimation with Sensitivity Analysis. *International Journal for Numerical Methods in Engineering* **69** (2007), 2219–2246.

[71] L. J. L. Nordström and T. P. Nordberg. "A critical comparison of time domain load identification methods". *Proceedings of the Sixth International Conference on Motion and Vibration Control.* Vol. 2. 2002, pp. 1151–1156.

[72] L. J. L. Nordström and T. P. Nordberg. A time delay method to solve non-collocated input estimation problems. *Mechanical Systems and Signal Processing* **18** (2004), 1469–1483.

[73] A. R. Plummer. Control techniques for structural testing: A review. *Proceedings of the Institution of Mechanical Engineers, Part I: Journal of Systems and Control Engineering* **221** (2007), 139–169.

[74] A. R. Plummer. "Modal Control for a class of Multi-Axis Vibration Table". *UKACC Control 2004 Mini Symposia.* 2004, pp. 111–115.

[75] A. D. Raath and C. C. van Waveren. A Time Domain Approach to Load Reconstruction for Durability Testing. *Engineering Failure Analysis* **5** (1998), 113–119.

[76] D. E. Roberts and N. C. Hay. Dynamic response simulation through system identification. *Journal of Sound and Vibration* **295** (2006), 1017–1027.

[77] J. D. Robson. Deductions from the Spectra of Vehicle Response due to Road Profile Excitation. *Journal of Sound and Vibration* **7** (1968), 156–158.

[78] J. D. Robson and C. J. Dodds. Stochastic Road Inputs and Vehicle Response. *Vehicle System Dynamics* **5** (1975), 1–13.

[79] H Ronasi. "Towards the Identification of Wheel-Rail Contact Forces". Chalmers University of Technology, 2010.

[80] C. Schedlinski. "Computational model updating of large scale finite element models". *Proceedings of the 18th International Modal Analysis Conference, IMAC.* 2000.

[81] "Virtual Nonlinear Multibody Systems". Ed. by W Schiehlen and M Valášek. V E Berbyuk. The Netherlands: Kluwer Academic Publishers, 2003. Chap. Control and Optimization of Semi-Passively Actuated Multibody Systems, pp. 279–295.

[82] B. Sevim, A. Bayraktar, and A. C. Altunisik. Finite element model calibration of berke arch dam using operational modal testing. *Journal of Vibration and Control* **17**.7 (2011), 1065–1079.

[83] G Shen et al. Implementation of electrohydraulic shaking table controllers with a combined adaptive inverse control and minimal control synthesis algorithm. *IET Control Theory and Applications* **5** (2010), 1471–1483.

[84] G Shen et al. Tracking control of an electro-hydraulic shaking table system using a combined feedforward inverse model and adaptive inverse control for real-time testing. *Proceedings of the Institution of Mechanical Engineers, Part I: Journal of Systems and Control Engineering* **225** (2011), 647–666.

[85] S Skogestad and I Postlethwaite. *Multivariable Feedback Control, analysis and design.* Chichester: John Wiley & Sons, 1996. ISBN: 0-471-94330-4.

[86] K Smolders, M Volckaert, and J Swevers. Tracking control of nonlinear lumped mechanical continuous-time systems: A model-based iterative learning approach. *Mechanical Systems and Signal Processing* **22** (2008), 1896–1916.

[87] US Department of Defence. *MIL-STD-810G Test Method Standard: Environmental Engineering Considerations and Laboratory Tests*. 2008.
[88] US Patent 5,623,402. *Multi-Channel Inverse Control Using Adaptive Finite Impulse Response Filters*. 1997.
[89] D Vaes. "Optimal Static Decoupling for Multivariable Control Design". PhD thesis. Katholieke Universiteit Leuven, 2005. ISBN: 90-5682-660-3.
[90] D Vaes, J Swevers, and P Sas. Experimental validation of different MIMO-feedback controller design methods. *Control Engineering Practice* **13** (2005), 1439–1451.
[91] D Vaes et al. Multivariable feedback design to improve tracking performance on tractor vibration test rig. *Mechanical Systems and Signal Processing* **21** (2007), 1051–1075.
[92] A Vepsä et al. Application of finite element model updating to a feed water pipeline of a nuclear power plant. *Nuclear Engineering and Design* **235**.17-19 (2005), 1849–1865.
[93] M. Vidyasagar. *Nonlinear Systems Analysis*. Englewood Cliffs, NJ: Prentice-Hall, 1993. ISBN: 0-89871-526-1.
[94] V. J. Virchis and J. D. Robson. Response of an Accelerating Vehicle to Random Road Undulation. *Journal of Sound and Vibration* **18** (1971), 423–427.
[95] B. Widrow and M. Bilello. "Adaptive Inverse Control". *Proceedings of the 1993 International Symposium on Intelligent Control*. 1993, pp. 1–6.
[96] P. Xu, G. Peticca, and D. Wong. A technique for developing a high accuracy durability test for a Light Truck on a Six Degree-of-Freedom Road Test Simulator. *International Journal of Vehicle Design* **47** (2008), 290–304.